PROCEEDINGS OF THE ROYAL SOCIETY A

rspa.royalsocietypublishing.org

Research

Cite this article: Ambrose DM, Bona JL, Nicholls DP. 2014 On ill-posedness of truncated series models for water waves. *Proc. R. Soc. A* **470**: 20130849.
http://dx.doi.org/10.1098/rspa.2013.0849

Received: 20 December 2013
Accepted: 27 February 2014

Subject Areas:
applied mathematics, computational mathematics, differential equations

Keywords:
water waves, Euler equations, ill-posedness, Dirichlet-to-Neumann

Author for correspondence:
David M. Ambrose
e-mail: ambrose@math.drexel.edu

On ill-posedness of truncated series models for water waves

David M. Ambrose[1], Jerry L. Bona[2] and David P. Nicholls[2]

[1]Department of Mathematics, Drexel University, Philadelphia, PA 19104, USA
[2]Department of Mathematics, Statistics and Computer Science, University of Illinois at Chicago, Chicago, IL 60607, USA

The evolution of surface gravity waves on a large body of water, such as an ocean, is reasonably well approximated by the Euler system for ideal, free-surface flow under the influence of gravity. The well-posedness theory for initial-value problems for these equations, which has a long and distinguished history, reveals that solutions exist, are unique, and depend continuously upon initial data in various function–space contexts. This theory is subtle, and the design of stable, accurate, numerical schemes is likewise challenging. Depending upon the wave regime in question, there are many different approximate models that can be formally derived from the Euler equations. As the Euler system is known to be well-posed, it seems appropriate that associated approximate models should also have this property. This study is directed to this issue. Evidence is presented calling into question the well-posedness of a well-known class of model equations which are widely used in simulations. A simplified version of these models is shown explicitly to be ill-posed and numerical simulations of quadratic- and cubic-order water-wave models, initiated with initial data predicted by the explicit analysis of the simplified model, lends credence to the general contention that these models are ill-posed.

1. Introduction

The Euler equations for ideal free-surface fluid mechanics (the water wave problem) are a standard model for the motion of large bodies of water (e.g. a lake or ocean) under the influence of gravity. With applications ranging

Royal Society Publishing

from tsunami propagation to sand bar formation to the interaction of ocean waves with oil rigs, these equations are of central importance for engineers, scientists and mathematicians alike.

Independently of the perspective one brings to their study, the question of the well-posedness of the Euler system is fundamental, viz. do solutions exist, are they unique, and do they depend continuously upon initial and boundary conditions? The pure initial-value problem for the full Euler system for free surface water wave propagation is known to be well-posed. Indeed, there is a long history associated with this problem which can be found reviewed in the recent works of Lannes [1] and Strauss [2]. Without going into details, the upshot of a very substantial development is that the water-wave problem is indeed well-posed in a variety of physically reasonable function classes.

When real applications are in view, it has been the case since the mid-nineteenth century that approximate models have come to the fore. Not only they are easier to deal with theoretically, but they also admit more robust numerical approximations which are important for their use in applications. One widely used family of model systems was introduced by Craig & Sulem [3]. Craig and Sulem started by writing the water wave evolution equations in the Zakharov formulation [4], which involves the Dirichlet-to-Neumann operator for the fluid domain. Using a theorem of Coifman & Meyer [5], one is able to expand the Dirichlet-to-Neumann operator as a series. Craig and Sulem make such an expansion, truncate the relevant series and use the resulting equations for simulations of the water wave problem.

Ambrose *et al*. [6] considered a class of weakly nonlinear, quadratic approximations of the Euler equations supplemented with an artificial viscosity. These models combine two primary ingredients: the method of operator expansions of Craig and Sulem and the artificial viscosity ideas put forward by Dias *et al.* [7]. In reference [6], it was established that if artificial viscosity effects are included, then the resulting model system is indeed well-posed in a reasonable range of function classes. However, the constants in the *a priori* energy-type estimates on which the theory depends vary in an unfortunate way upon the viscosity parameter. This is not surprising. What did cause pause was that more detailed analysis did not yield bounds which can be controlled as the viscosity vanishes. We then considered the possibility that inviscid models, constructed in the spirit of Craig and Sulem, may not actually be well posed.

Further investigation with a change of perspective has thrown up evidence that in fact, these inviscid models are *ill*-posed. This evidence is as follows: first, it is shown that a reduced version of the quadratic model is ill-posed, because it does not feature continuous dependence of solutions upon initial data. Indeed, it is shown, for the reduced model, that there is a sequence of initial data (indexed by integers $J \to \infty$) of size C/J (in an appropriate function space) that produce solutions which blow-up at a time proportional to $1/J$. Once this ill-posedness result is in hand, we return to the full truncated quadratic and cubic models and initiate them with the data that produced singularity formation for the reduced model. This family of initial data is uniformly bounded in the Sobolev space H^1, and goes to zero in H^s for any $s < 1$. Our numerical experiments in this circumstance display blow-up in a time proportional to $1/J$, suggesting that the same mechanism for ill-posedness holds for the quadratic and cubic models as it does for the reduced model. To forestall the idea that the ill-posedness is connected solely with the roughness of the initial data, further simulations were performed using two other families of initial data: one of which is uniformly bounded in $H^{3/2}$ and goes to zero in H^s for any $s < 3/2$, and another which is uniformly bounded in $H^{5/2}$, and which goes to zero in H^s for any $s < 5/2$. We again found numerical evidence of ill-posedness.

The conclusion drawn from these machinations is that one must take care using operator expansions and truncation to produce models for water wave propagation. It is not necessarily the case that this technique preserves the structure of the original equations that allow for a well-posedness theory (see [8,9] for instances of this phenomenon in a shallow-water setting). In future work, we will endeavour to redesign such truncated series models, taking into account the well-posedness theory for water waves, with the goal of arriving at systems which are well-posed, but which also maintain the attractive features of the truncated series models, such as ease of numerical simulation (see again [8,9] in the shallow-water context).

The rest of the paper is organized as follows: in §2, the quadratic and cubic models considered here are reviewed. In §3, a reduced model is introduced which focuses on two terms in the quadratic model that appear to be connected to ill-posedness. This reduced model is shown directly to be ill-posed. In §4, numerical evidence is presented of the ill-posedness for the full quadratic and cubic-truncated models, using the information gleaned from the analysis of the reduced model. We close in §5 with a summary and a discussion. A brief sketch of the derivation of the truncated models from the full Euler system is shown in appendix.

2. Water wave models

We consider the problem of gravity waves for an ideal, irrotational fluid satisfying the incompressible Euler equations. The wave motion is assumed to be long-crested, so that a two-dimensional description is appropriate. The spatial coordinates (x, y) are chosen, so that y increases in the direction opposite to which gravity acts, and $\{(x, y) : y = 0\}$ corresponds to the rest position of the fluid. At time t, the fluid domain is $\{(x, y) \in \mathbb{R}^2 : y < \eta(x, t)\}$, which is to say, the function $\eta(x, t)$ is the deviation of the free fluid surface from its rest position, and the fluid is infinitely deep. Of course, this presumes that the deviation η of the fluid surface is a single-valued function of x, an assumption that we make throughout. Because the flow is irrotational and incompressible, there is a velocity potential, $\varphi(x, y, t)$, which satisfies $\Delta\varphi(x, y, t) = 0$, for all (x, y) in the fluid domain. Using the Dirichlet-to-Neumann operator for the fluid domain (with normal vector N),

$$G := \nabla\varphi(x, \eta) \cdot N = \partial_y\varphi(x, \eta) - (\partial_x\eta)\partial_x\varphi(x, \eta),$$

the Euler system can be described entirely in terms of the surface quantities $\eta(x, t)$ and $\xi(x, t) = \varphi(x, \eta(x, t), t)$. The motion is taken to be periodic of period 2π in the x-direction, so that $\eta(x + 2\pi, t) = \eta(x, t)$ and $\xi(x + 2\pi, t) = \xi(x, t)$, for all x and t. The full Euler system for the motion in these circumstances appears in appendix. As mentioned in §1, the full water-wave problem is theoretically and numerically recalcitrant. It is very often the case that truncated models are used when applications are in view.

Interest is focused on the question of well-posedness or ill-posedness of the truncated system

$$\eta_t = \Lambda\xi - \partial_x\{[H, \eta]\Lambda\xi\} \tag{2.1a}$$

and

$$\xi_t = -g\eta + \tfrac{1}{2}(\Lambda\xi)^2 - \tfrac{1}{2}(\xi_x)^2, \tag{2.1b}$$

which is here referred to as the WW2 model. (Read this as 'water-wave 2' model, where the 2 refers to the fact that terms in the operator expansion of at most quadratic order are being kept; details of the derivation of this model are included in appendix.) The constant g is the acceleration owing to gravity, and the operator Λ is $\Lambda = H\partial_x$, where H connotes the periodic Hilbert transform. The Fourier symbol $\hat{\Lambda}(k)$ of Λ is $|k|$. The operator $[H, \eta]$ is a commutator: given a function f, we have $[H, \eta]f = H(\eta f) - \eta H(f)$.

Also treated in our numerical simulations is the third-order approximation

$$\partial_t\eta = \Lambda\xi - \partial_x[\eta\partial_x\xi] - \Lambda[\eta\Lambda\xi] - \partial_x\left[\left(\frac{\eta^2}{2}\right)\partial_x\Lambda\xi\right] - \Lambda\left[\left(\frac{\eta^2}{2}\right)\Lambda^2\xi\right] - G_1(\eta)[\eta\Lambda\xi] \tag{2.2a}$$

and

$$\partial_t\xi = -g\eta - \left(\frac{1}{2}\right)\{(\partial_x\xi)^2 - (\Lambda[\xi])^2\} + (\Lambda\xi)\{\partial_x[\eta\partial_x\xi] - \Lambda[\eta\Lambda\xi] + (\partial_x\xi)(\partial_x\eta)\}. \tag{2.2b}$$

to the water-wave problem, obtained by keeping one more order in the operator expansion (see again appendix). This system is referred to as WW3.

It is conjectured that the periodic initial-value problems for both of the above systems are ill-posed. Evidence in the direction of this conjecture begins with a study of the reduced model

$$v_t = (\Lambda v)^2 - (v_x)^2. \tag{2.3}$$

The right-hand side of the reduced model appears on the right-hand side of (2.1*b*) and (2.2*b*), and we suspect that these are the terms leading to ill-posedness of the initial-value problems for both WW2 and WW3. To be more precise, the term $(\Lambda\xi)^2$, which can be viewed as a parabolic term of indefinite sign, appears to be the cause of the trouble. Incidentally, we are *not* proposing (2.3) as a new model of water-waves, but are simply using it to help understand the dynamics of solutions of (2.1) and (2.2).

3. Ill-posedness of the reduced model

The analysis begins by writing the Fourier series representation

$$v(x,t) = \sum_{k=-\infty}^{\infty} v_k(t)\, \mathrm{e}^{\mathrm{i}kx} \tag{3.1}$$

of the solution, assuming that it lies in L^2 as a function of x on a period domain, for almost every t. Combining (2.3) with (3.1) yields the evolution equations

$$\frac{\mathrm{d}}{\mathrm{d}t} v_k = \sum_{\ell=-\infty}^{\infty} [|(k-\ell)\ell| + (k-\ell)\ell] v_{k-\ell} v_\ell \tag{3.2}$$

for the Fourier coefficients v_k. Note that the factor $|(k-\ell)\ell| + (k-\ell)\ell$ appearing in brackets is non-negative. This suggests using the idea put forth in reference [10] in the study of blow-up solutions for the periodic complex Korteweg–de Vries (KdV) equation. Consider coefficients v_k which are such that $v_k = v_{-k}$ and $v_k \geq 0$ for all k. It is clear from (3.2) that if $v_k(0) \geq 0$ and $v_k = v_{-k}$ for all k, then these properties will continue to hold for $t > 0$. (This amounts to considering cosine series with non-negative coefficients in the representation (3.1).) For $s > 0$, take the norm in the Sobolev space $H^s = H^s([0, 2\pi])$ to be

$$\|v\|_{H^s} = \left(\sum_{k=0}^{\infty} (1 + k^{2s}) v_k^2 \right)^{1/2}.$$

This is equivalent to the usual H^s-norm for functions with even, real Fourier coefficients.

Note that for a given value of k, for all but finitely many values of ℓ, the quantity in brackets in (3.2) will be zero. More precisely, the sum on the right-hand side of (3.2) can be rewritten as

$$\frac{\mathrm{d}}{\mathrm{d}t} v_k = v_{k,t} = \sum_{\ell=1}^{k-1} [|(k-\ell)\ell| + (k-\ell)\ell] v_{k-\ell} v_\ell = \sum_{\ell=1}^{k-1} [2(k-\ell)\ell] v_{k-\ell} v_\ell. \tag{3.3}$$

In more detail, we have the following for small values of k:

$$v_{0,t} = 0, \quad v_{1,t} = 0, \quad v_{2,t} = 2v_1^2, \quad v_{3,t} = 8v_1 v_2,$$
$$v_{4,t} = 12 v_1 v_3 + 8 v_2^2, \quad v_{5,t} = 16 v_1 v_4 + 24 v_2 v_3, \ldots$$

The stage is set to show that solutions of the reduced model can blow up arbitrarily quickly for arbitrarily small initial data. This is the content of theorem 3.1.

Theorem 3.1. *For any $s \in [0, 2)$, the initial-value problem for the reduced model* (2.3) *is ill-posed in the Sobolev space H^s. Specifically, there is a family of initial data $v_0^{(J)} \in H^s$ with $\left\| v_0^{(J)} \right\|_{H^s} \to 0$ as $J \to \infty$, such that the corresponding solutions of the initial-value problem blow up in H^s by time T_J, where $T_J \to 0$ as $J \to \infty$.*

Proof. For fixed $s \in [0,2)$ and $J \in \mathbb{N}$, define the initial condition $v_0 = v_0^{(J)}$ via its Fourier coefficients, viz.

$$v_{0,J}^{(J)} = v_{0,-J}^{(J)} = c > 0, \quad v_{0,k}^{(J)} = 0, \text{ for all } k \neq \pm J.$$

Let $v = v^J$ connote the solution of (3.2) emanating from the initial data $v_0^{(J)}$ and denote the Fourier coefficients of $v = v^J$ by $\{v_k = v_k^J\}_{k\in\mathbb{Z}}$. (As J is fixed for the moment, the superscript J is suppressed for ease of reading in the next few paragraphs.)

The temporal dependence of the Fourier coefficients of v is now estimated. Because, for all k, $(\mathrm{d}/\mathrm{d}t)v_k = v_{k,t} \geq 0$, it follows that $v_J(t) = v_{-J}(t) \geq c$ for all $t > 0$ for which the solution exists. Focusing upon $k = 2J$ and $\ell = J$ in (3.3), it is seen immediately that $v_{2J,t} \geq 2J^2(v_J)^2$, whence $v_{2J}(t) \geq 2J^2c^2t$. Next, using again the non-negativity of the Fourier coefficients and considering the case $k = qJ$, $\ell = J$ and $\ell = qJ - J$ in (3.3), it is readily deduced that

$$\frac{\mathrm{d}}{\mathrm{d}t} v_{qJ} \geq 4J^2(q-1)v_J v_{(q-1)J}, \text{ for all } q \geq 2. \tag{3.4}$$

We claim that for all $k \geq 2$, $v_{kJ}(t) \geq 2(4^{k-2})J^{2(k-1)}c^k t^{k-1}$. This will be proved by induction, the case $k = 2$ being in hand. Assume that the claim is true for $k = m$, which is to say, $v_{mJ}(t) \geq 2(4^{m-2})J^{2(m-1)}c^m t^{m-1}$. Use (3.4) with $q = m+1$ together with the induction hypothesis about v_{mJ} to find that

$$\frac{\mathrm{d}}{\mathrm{d}t} v_{(m+1)J} \geq 4J^2(m)v_J v_{mJ} \geq 2(4^{m-1})mJ^{2m}c^{m+1}t^{m-1}.$$

Integrating this inequality over $[0,t]$ reveals that $v_{(m+1)J}(t) \geq 2(4^{m-1})J^{2m}c^{m+1}t^m$, thereby validating the claim.

In consequence of the these lower bounds, it must be the case that for all $k \geq 2$,

$$v_{kJ}(t) \geq 2(4^{k-2})J^{2(k-1)}c^k t^{k-1} = \frac{c}{2}(4J^2ct)^{k-1}.$$

This implies that by time $t = 1/4J^2c$, v fails to be in L^2 since by that time, infinitely many of its Fourier coefficients are greater than or equal to the positive constant $c/2$. The solution v is thus seen to remain in L^2 on a maximal time interval $[0, T_*)$ with $T_* \leq 1/4J^2c$.

The constant c is now chosen in a helpful way. Let α and β be positive constants and choose $c = c_J = \alpha/J^\beta$. The norm of the initial data is then $\|v(\cdot,0)\|_{H^s} = \|v_0^{(J)}\|_{H^s} = \alpha((1+J^{2s})/J^{2\beta})^{1/2}$, and the solution must blow up in L^2 before time $1/4\alpha J^{2-\beta}$. Choosing α and β, so that $\alpha > 0$ and $s < \beta < 2$, we conclude that arbitrarily small data yield solutions which blow up arbitrarily quickly. This establishes lack of continuous dependence on the initial data for the initial-value problem. ■

Remark 3.2. At the end of the above proof, if $\alpha = 1/2$ and $\beta = 1$, then the solution of the initial-value problem with data $v(x,0) = (1/J)\cos(Jx)$ is seen to blow up in time proportional to $1/J$. In §4, numerical simulations of the full WW2- and WW3-truncated models are run using three families of initial data; one of these families corresponds to this choice, $v(x,0) = (1/J)\cos(Jx)$. Specifically, we will report the results of simulations of the WW2 and WW3 models using the data

$$\eta(x,0) = 0, \quad \xi(x,0) = \frac{1}{J}\cos(Jx). \tag{3.5}$$

The second family of data corresponds to $\alpha = 1/2$ and $\beta = 3/2$, which is to say, to $v(x,0) = (1/J^{3/2})\cos(Jx)$. For the WW2 and WW3 models, this means that the second family of initial data used in the simulations is

$$\eta(x,0) = 0, \quad \xi(x,0) = \frac{1}{J^{3/2}}\cos(Jx). \tag{3.6}$$

The same type of blow-up behaviour seen for the reduced model is evident in these simulations of the WW2 and WW3 systems. Note that for both of these choices of data, $\eta(x,0)$ is obviously analytic. With the choice (3.5), $\xi(\cdot,0)$ is bounded in H^1, and goes to zero in H^s for any $s < 1$ as $J \to \infty$. With the choice (3.6), $\xi(x,0)$ is uniformly bounded in $H^{3/2}$, and goes to zero in H^s for any $s < 3/2$ as $J \to \infty$.

The reduced model is certainly ill-posed in all Sobolev spaces, but the above proof demonstrates ill-posedness in H^s only for $s < 2$. The proof takes one pair of Fourier modes to be initially non-zero. The result can improved by making different choices of the non-zero Fourier modes of the initial data. To get an idea of what is possible, another choice of initial data is made that provides ill-posedness of the reduced model in H^s for $s < 3$.

Theorem 3.3. *For any $s \in [0, 3)$, the initial-value problem for the reduced model* (2.3) *is ill-posed in the Sobolev space H^s. Specifically, there is a sequence $\{v_0^{(J)}\}_{J=1}^{\infty}$ of initial data with $v_0^{(J)} \to 0$ in H^s as $J \to \infty$, having the property that the corresponding solutions of the initial-value problem blow up in H^s by time T_J, where $T_J \to 0$ as $J \to \infty$.*

Proof. Fix $s \in [0, 3)$ and $J \in \mathbb{N}$ and define initial data $v_0^{(J)}$ via its Fourier coefficients, viz.

$$v_{0,1} = v_{0,-1} = b > 0, \quad v_{0,J} = v_{0,-J} = c > 0, \quad v_{0,k} = 0, \text{ otherwise.}$$

As noted previously, if $\{v_k\}_{k\in\mathbb{Z}}$ are the Fourier coefficients of the solution v starting at $v_0^{(J)}$, then $(\mathrm{d}/\mathrm{d}t)v_1 = 0$ and $(\mathrm{d}/\mathrm{d}t)v_J \geq 0$. It is therefore concluded that $v_1(t) = b$ and $v_J(t) \geq c$ for all t in the time interval of existence of the solution. Considering $k = J + 1$ and $\ell = 1$ in (3.3) yields the inequality

$$\frac{\mathrm{d}}{\mathrm{d}t} v_{J+1} \geq 2J v_J v_1 \geq 2Jbc.$$

Integrating this inequality in time gives $v_{J+1}(t) \geq 2Jbct$ for all t. Next, consider $k = 2J + 1$ and $\ell = J$ in (3.3) to find the inequality

$$\frac{\mathrm{d}}{\mathrm{d}t} v_{2J+1} \geq 2(J+1)J v_{J+1} v_J \geq 4J^3 bc^2 t,$$

which implies immediately that

$$v_{2J+1} \geq 2J^3 bc^2 t^2. \tag{3.7}$$

Consider $k = (q + 1)J + q$ with $q = 1, 2, \ldots$ and seek to prove by induction that

$$v_{(q+1)J+q} \geq c(2t^2 J^3 bc)^q. \tag{3.8}$$

Note that (3.7) serves to establish the base case $q = 1$ for the induction. Given $m > 1$, assume that $v_{(m+1)J+m} \geq c(2t^2 J^3 bc)^m$. Choose $k = (m + 2)J + (m + 1)$ and $\ell = J + 1$ and use (3.3) to conclude that

$$\frac{\mathrm{d}}{\mathrm{d}t} v_{(m+2)J+(m+1)} \geq 2((m+1)J + m)(J+1) v_{(m+1)J+m} v_{J+1} \geq 2(m+1)J^2 v_{(m+1)J+m} v_{J+1}.$$

Substituting from the lower bounds on $v_{(m+1)J+m}$ and v_{J+1} allows the latter inequality to be extended thusly

$$\begin{aligned}\frac{\mathrm{d}}{\mathrm{d}t} v_{(m+2)J+(m+1)} &\geq 2(m+1)J^2 (2Jbct)(c)(2t^2 J^3 bc)^m \\ &= 2^{m+1}(2m+2)J^{3m+3}(c)c^{m+1}b^{m+1}t^{2m+1}.\end{aligned}$$

Integrating with respect to t provides the lower bound

$$v_{(m+2)J+(m+1)} \geq 2^{m+1} J^{3m+3}(c)c^{m+1}b^{m+1}t^{2m+2} = c(2J^3 bct^2)^{m+1}, \tag{3.9}$$

thereby completing the induction and establishing the inequality (3.8) for all $q \geq 1$.

From (3.8), it follows that the solution v has certainly blown up in L^2 (just as in the previous proof) if the quantity in parentheses on the right-hand side of (3.8) is equal to one. This means the solution exists on the time interval $[0, T_*)$ with $T_*^2 \leq 1/2J^3 bc$.

The H^s-norm of the initial data is $(2b^2 + (1 + J^{2s})c^2)^{1/2}$. Take $b = \alpha J^{-\beta}$ and $c = \gamma J^{-\delta}$ with α, β, γ and δ all positive. Choose $\alpha = \gamma = 1/2$ and seek β and δ such that $s - \delta < 0$ and $3 - \beta - \delta > 0$. The condition on $3 - \beta - \delta$ ensures that $T_* \to 0$ as $J \to \infty$, whereas $s - \delta < 0$ ensures that the H^s-norm of the initial data goes to zero as $J \to \infty$. Because $s < 3$, the choice $\delta = (3 + s)/2$ and $\beta = (3 - s)/4$ meets all the criteria. The proof is complete. ∎

Remark 3.4. As we mentioned in remark 3.2, three families of initial data are used in the simulations of the WW2 and WW3 models in §4. The third family of initial data is related to the data arising in the proof of theorem 2 with the choices $\alpha = 1/2, \beta = 1/10, \gamma = 1$ and $\delta = 5/2$. More specifically, we will compute using the initial data

$$\eta(x,0) = 0, \quad \xi(x,0) = \frac{1}{J^{1/10}}\cos(x) + \frac{2}{J^{5/2}}\cos(Jx). \tag{3.10}$$

The prediction from the reduced model is that the corresponding solution will blow up in time proportional to $J^{-1/5}$ (or faster). Note that with this choice, $\xi(\cdot,0)$ is uniformly bounded in $H^{5/2}$ and goes to zero in H^s, for all $s < 5/2$, as $J \to \infty$.

We expect similar ill-posedness results hold for the reduced system in higher-regularity spaces. This point has not been pursued, however. We were content with the results of ill-posedness in hand together with the numerically obtained evidence reported in §4.

4. Ill-posedness for the water-wave models

To bolster the conjecture that the quadratic WW2, (2.1) and cubic WW3, (2.2), truncated series models for water waves feature ill-posed initial-value problems, the results of some numerical simulations are presented. These are initiated with initial conditions inspired by our calculations showing that the reduced model (2.3) is ill-posed. The simulations are accomplished using a Fourier collocation method for the spatial discretization with a standard fourth-order Runge–Kutta scheme for the time-stepping [11].

In more detail, for the 2π-periodic problem, solutions $\{\eta(x,t), \xi(x,t)\}$ of (2.1) and (2.2) are approximated by their truncated Fourier series, viz.

$$\eta^{N_x}(x) = \sum_{k=-N_x/2}^{N_x/2-1} \hat{\eta}_k^{N_x} \mathrm{e}^{\mathrm{i}kx} \quad \text{and} \quad \xi^{N_x}(x) = \sum_{k=-N_x/2}^{N_x/2-1} \hat{\xi}_k^{N_x} \mathrm{e}^{\mathrm{i}kx}.$$

These approximations are inserted into (2.1) and (2.2) and equality enforced at the equally spaced gridpoints $x_j = 2\pi j/N_x$. This leads to a coupled system of $2N_x$ ordinary differential equations which are supplemented with $2N_x$ initial conditions obtained by demanding that the value of the discrete initial data matches that of the continuous initial values at the grid points x_j, $-N_x/2 \le j \le N_x/2 - 1$. This system of ordinary differential equations is solved with a classical fourth-order, Runge–Kutta temporal integration.

Two aspects of this fully discrete approximation deserve further comment. First, in solving (2.1) and (2.2), one must simulate the Fourier multiplier $\Lambda = H\partial_x$. This is straightforward for a Fourier collocation method, because in the Fourier transformed variables, Λ is simply multiplication by $|k|$ for all wavenumbers k. Consequently, we set

$$\Lambda\eta^{N_x}(x) = \sum_{k=-N_x/2}^{N_x/2-1} |k|\hat{\eta}_k^{N_x} \mathrm{e}^{\mathrm{i}kx}.$$

Second, as we are expecting singularity formation, experience indicates that it is important to filter the solution sufficiently, so that it is clear that any observed growth is due to the mechanisms of the model system rather than the artificial amplification of discretization errors. This is accomplished with a standard 'low-pass filter' of the form

$$\mathcal{S}_P[\eta^{N_x}(x)] = \sum_{k=-P}^{P} \hat{\eta}_k^{N_x} \mathrm{e}^{\mathrm{i}kx},$$

which is applied to the approximations of the dependent variables after every timestep. The parameter P is determined by experience, but variations of the approximations with variations in P are investigated and reported below.

(a) Convergence studies

To provide confidence in the numerical results outlined below, a straightforward convergence study is conducted. As we do not know any helpful exact solution of the systems (2.1) or (2.2), the convergence analysis is based upon the small, smooth initial conditions

$$\eta(x,0) = A\cos(kx), \quad \xi(x,0) = -\frac{A\omega_k}{|k|}\sin(kx), \quad \omega_k := \sqrt{g|k|}.$$

For integer k, these initial conditions generate 2π-periodic, travelling-wave solutions of the *linear* water wave problem WW1, namely

$$\eta_t = \Lambda\xi, \quad \xi_t = -g\eta.$$

The expectation is that this initial data should generate well-behaved solutions in the WW2 and WW3 models. In our simulations, we selected $g = 1$ and $A = 1/100$.

Consider a more or less fully resolved approximation, denoted (η_f, ξ_f), corresponding to these initial conditions and evolved to a final time $T = \pi/2$ using a very fine resolution (in this instance $N_x = 1024$ collocation points and $N_t = 10\,240$ time steps). Two experiments are reported.

1. For a fixed number of collocation points (here we choose $N_x = 32$) and a selection of numbers of timesteps $N_t = 16, 24, 32, \ldots, 512, 768$, compute the relative difference in supremum norm between the associated solutions (η, ξ) and (η_f, ξ_f) at the final time T. Here, the convergence in the temporal variable is being checked.
2. For a fixed number of timesteps (here we choose $N_t = 4000$) and a selection $N_x = 4, 6, 8, \ldots, 18, 20$, of collocation points, determine the relative difference between the associated solutions (η, ξ) and (η_f, ξ_f) at the final time T in the supremum norm. The spatial convergence of the scheme is being tested in this experiment.

In all cases (the high fidelity run and the coarser experiments), the discretization parameters satisfied the Courant–Friedrichs–Lewy (CFL) condition for stability [11].

Figure 1 displays results derived from the first set of experiments, whereas figure 2 shows the outcome of the second. Both experiments revealed rapid convergence of the numerical simulations of these smooth solutions, with errors on the order of machine precision. (The flattening out of the error in figure 2 at about 10^{-14} is an indication of an overall condition number for our algorithm of about 100.)

A linear least-squares fit of the logarithm of the error observed in the first set of experiments versus the logarithm of N_t gives slopes of -3.995 and -3.994 for WW2 and WW3, respectively, suggesting the fourth-order convergence one expects of the classical Runge–Kutta scheme used here. The spatial convergence results in figure 2 exhibit a linear behaviour when its logarithm is plotted versus the number of collocation points, which is consistent with the exponential rate of convergence one hopes for when using Fourier collocation.

(b) Numerical study of ill-posedness

This section is devoted to report the outcome of particular computer simulations of solutions of the periodic initial-value problems for the WW2 and WW3 models. It will be seen that the exact results regarding ill-posedness of the reduced model (2.3) apparently have counterparts for the full models.

The 2π-periodic auxiliary data featured in remarks 3.2 and 3.4 (see (3.5), (3.6) and (3.10)) are used to initiate the numerical simulations. The growth of the L^∞-norms of the resulting approximate solutions under the evolutions WW2 and WW3 is then studied. The simulations were run out to time $T = \pi$ (though in the event, none of the simulations continued this long). We

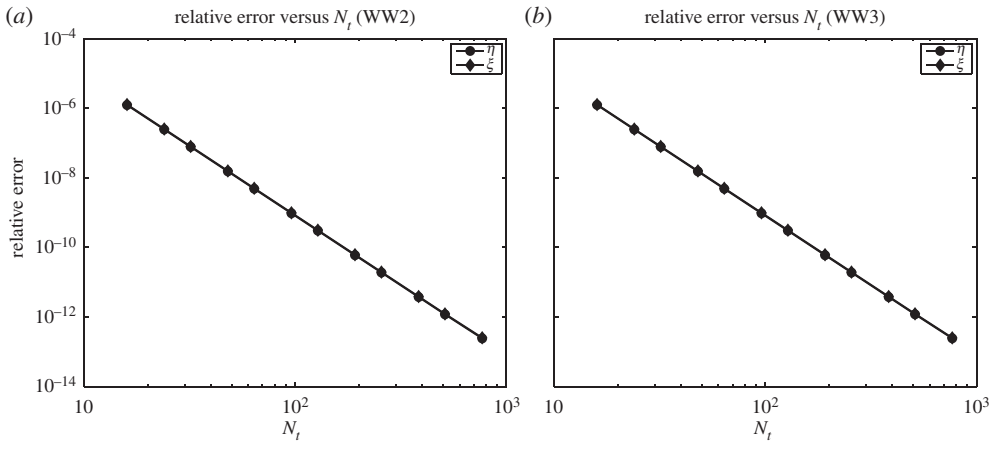

Figure 1. Plots of the relative error (supremum norm) at the final time $T = \pi/2$ versus the number of timesteps N_t of numerical approximations of the system of equations WW2 (*a*) and WW3 (*b*). The errors for η and ξ are nearly identical, so the data points are almost indistinguishable.

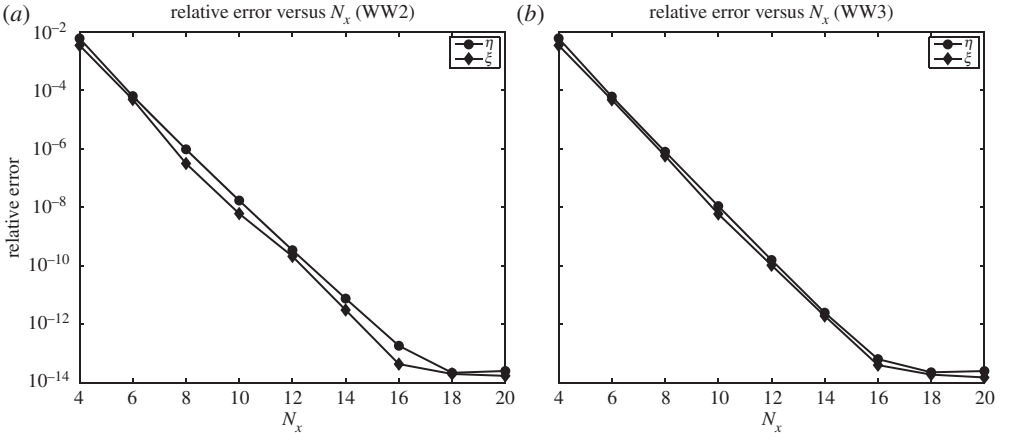

Figure 2. Plots of the relative error (supremum norm) at $T = \pi/2$ versus the number of collocation points N_x of numerical approximations of the model systems WW2 (*a*) and WW3 (*b*).

considered pairs (N_x, N_t) in the ranges $200 \leq N_x \leq 4000$ and, for each run we took N_t so that

$$\lambda = \frac{\Delta t}{\Delta x} = \frac{T}{L}\frac{N_x}{N_t} = \frac{1}{2}\frac{N_x}{N_t} \approx \frac{1}{2}, \tag{4.1}$$

thereby satisfying the CFL condition for the linearized system. For each simulation, the L^∞-norm is monitored, and the first time $t = t^*(N_x)$ for which a predetermined tolerance is exceeded is recorded. For the first set of simulations reported, this tolerance is taken to be 10^4. The times $t^*(N_x)$ are then averaged over the values of N_x selected and the result denoted T^*. This average time T^* is referred to informally as the 'blow-up' time. Of course, the blow-up times depend upon the initial data.

In all of our experiments, the L^∞-norm of the computed solution (η, ξ) reached the prescribed tolerance rather quickly, certainly indicating a lack of global well-posedness. In particular, the blow-up times corresponding to smaller and smaller initial data exceeded the specified tolerance at times that were bounded above. The conclusion drawn from this state of affairs is that

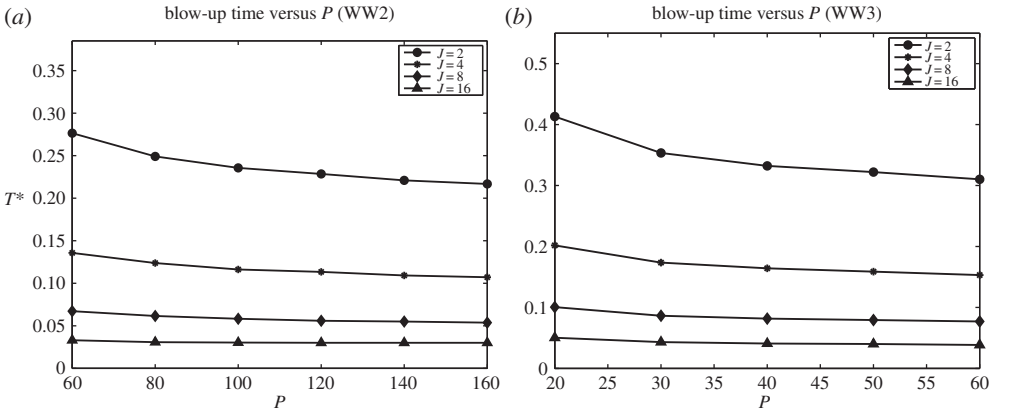

Figure 3. Plot of the blow-up times T^* versus the filtering parameter P for the initial conditions (3.5) in the water wave models WW2 (*a*) and WW3 (*b*).

arbitrarily small initial data leads to solutions that, at a fixed positive time, are bounded away from zero. This shows lack of continuity with respect to the initial data and so ill-posedness. In one spatial dimension, the H^r-norm controls the L^∞-norm for any $r > 1/2$. Thus, if the L^∞-norm is not small, then the H^r-norm cannot be small, either. Hence, ill-posedness in certain Sobolev norms is also inferred. In most of the simulations which follow, the blow-up times actually go to zero as the data gets smaller, just as they did for the reduced model.

A more detailed description of the outcome of our numerical simulations is now entered upon. Consider first initial data as suggested in remark 3.2, equation (3.5), namely

$$\eta(x,0) = 0 \quad \text{and} \quad \xi(x,0) = \frac{1}{J}\cos(Jx).$$

The initial data were run with $J = 2, 4, 8, 16$ and with values of the Fourier filtering set at $P = 60J, 70J, \ldots, 160J$. The amplitude tolerance was 10^4, and we ran our scheme for the WW2 system with values of N_x from 200 to 2000 in increments of 200 and associated values of N_t satisfying (4.1) to determine the blow-up times. Figure 3*a* shows results of these experiments. As expected, the blow-up times T^* decrease somewhat as P increases. (This would likely cease to be true if PJ got near to N_x, as aliasing would set in.) The fact that the blow-up times appear to be settling down as P is increased adds confidence that what we are seeing is the real state of affairs for the differential equations and not some artefact of the numerical scheme. A linear least-squares fit to a power law of the logarithm of J to the logarithm of the blow-up times T^*, all computed using the largest value of the filtering parameter P, yields

$$T^* = CJ^p, \tag{4.2}$$

where $p = -0.955485$. A companion computation with the same initial data (3.5), but used to initiate WW3, gives results which are very similar to those for the WW2 model. These are displayed in figure 3*b*. The WW3 simulations use a finer discretization in the spatial variable, viz. N_x ran from 2000 to 4000 in increments of 400 and different filter values, $P = 20J, \ldots, 60J$ were used. Conducting the least-squares fit of the log of the blow-up time to the log of J in (4.2) yields $p = -1.00256$.

Studied also was the second family of initial conditions,

$$\eta(x,0) = 0, \quad \xi(x,0) = \frac{1}{J^{3/2}}\cos(Jx),$$

appearing in remark 3.2 (see formula (3.6)) for $J = 4, 8, 16$, $P = 60J, \ldots 160J$. The amplitude tolerance was again set to 10^4, and the values of N_x used to determine the blow-up times were the

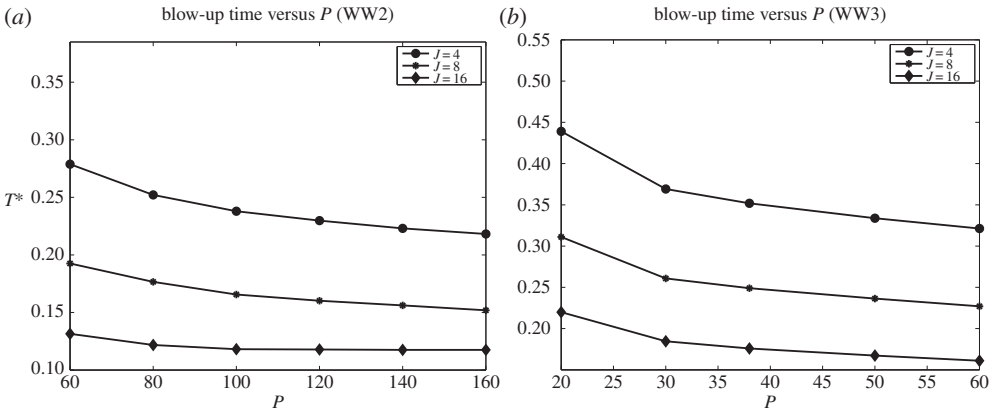

Figure 4. Plot of blow-up time T^* versus the filtering parameter P for the initial conditions (3.6) in the water wave models WW2 (*a*) and WW3 (*b*).

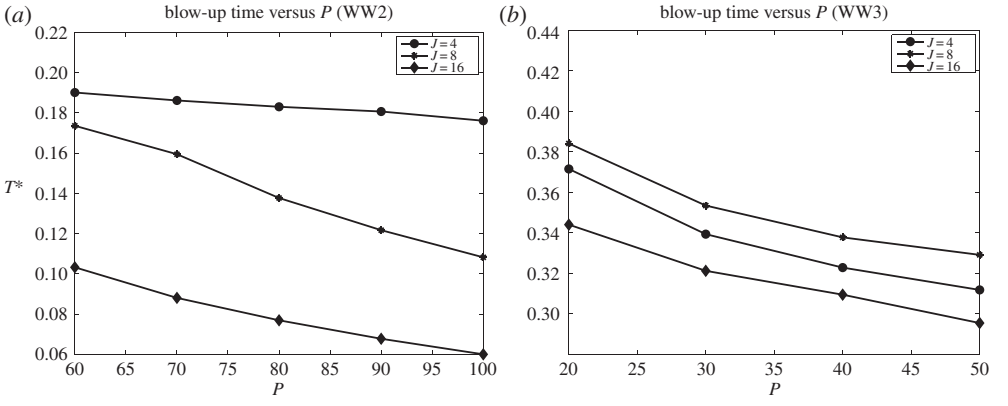

Figure 5. Plot of order-one time T^* versus the filtering parameter P for the initial conditions (3.10) in the water wave models WW2 (*a*) and WW3 (*b*).

same as in the experiments corresponding to figure 3. The computed blow-up times are displayed in figure 4 for these initial conditions evolved in WW2 (figure 4*a*) and WW3 (figure 4*b*). Least-squares fits to the value p in (4.2) yield $p = -0.446468$ in WW2 and $p = -0.498238$ for WW3. (For the WW3 simulation, the finer discretization in the spatial variable and the filter values applied in the previous WW3 simulation were used.)

Simulations were also made with the initial conditions

$$\eta(x,0) = 0, \quad \xi(x,0) = \frac{1}{J^{1/10}}\cos(x) + \frac{2}{J^{5/2}}\cos(Jx),$$

put forward in remark 3.4, equation (3.10). These simulations featured $J = 4, 8, 16$, N_x running from 2000 to 4000 in increments of 400 and $P = 60J, \ldots 100J$. Here, the blow-up occurs much more slowly, no doubt because as J increases, such initial data become small in smaller Sobolev spaces than does the data in (3.5) and (3.6). Particularly in WW3, the growth of the L^∞-norm, while inexorable, is quite slow. Consequently, the blow-up tolerance was reduced to 10. Thus, the simulation discovers when small initial data lead to more than an order of magnitude increase in size. Results are plotted in figure 5 for initial conditions evolved in WW2 (figure 5*a*) and WW3 (figure 5*b*). Least-squares fits to the value p in (4.2) yield $p = -0.77552$ and $p = -0.0388835$.

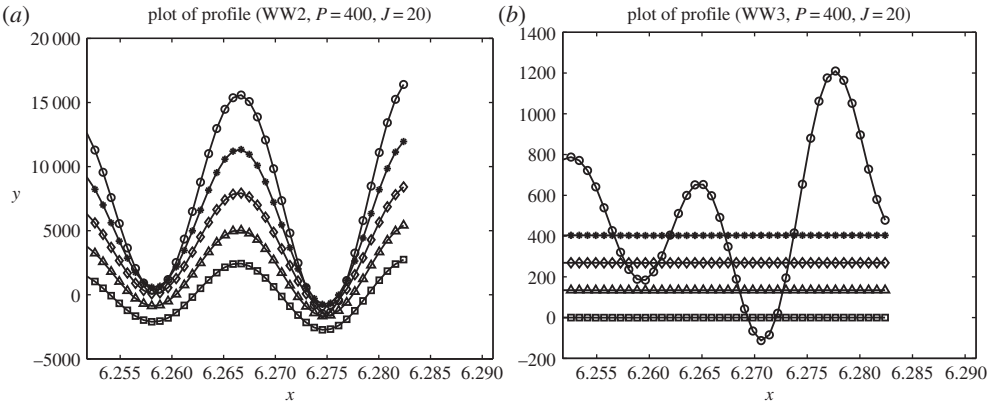

Figure 6. (*a*, *b*) Plot of solution profiles in the five timesteps before the blow-up time T^* in the water wave models WW2 and WW3.

This section ends with two plots of the *physical profile* of one of these waveforms, just prior to it reaching the 'blow-up' tolerance. For this, we focus upon the simplest initial conditions, namely those in (3.5). Figure 6 depicts the computed approximation in the five timesteps immediately preceding T^* in WW2 (figure 6*a*) and WW3 (figure 6*b*). In both these graphs, we have zoomed in on the right spatial endpoint where the solution is growing rapidly. Note how quickly the amplitude is increasing! This simulation was done with $N_x = N_t = 8000$ where λ in (4.1) is 1/2. The timestep is about 0.0004, so the growth is explosive. Note also the rapid oscillations and the highly resolved nature of our numerical simulation (the spatial discretization is about 0.0008). For the simulation made using the WW3 model, not only does the final profile display oscillations, the four prior to that do as well, though their structure is too small to see on the scale used to make the plot.

5. Discussion

Considered here have been truncated series models for deep-water, free-surface waves. Our analysis, while not definitive, indicates that the initial-value problems for these models are in fact ill-posed. The evidence in favour of this proposition is two-fold. First, a reduced model is shown to be ill-posed in smooth function classes. Second, the data that reveal ill-posedness of the reduced model, when used to initiate a numerical scheme for the full truncated models at second- and third-order, reveal the same sort of ill-posedness that is obtained for the reduced model.

In the light of these results, it is natural to ask whether the inclusion of physical effects heretofore ignored in the truncated series models might remedy ill-posedness. The authors have previously shown in reference [6] that the inclusion of viscous terms does lead to WW2 becoming well-posed. While such viscous terms are artificial, they are commonly used in applications and have at least some physical motivation (see [7]). Alternatively, one may ask whether the inclusion of higher-order dispersive effects, such as surface tension, might lead to well-posed initial-value problems.

The issue of whether or not surface tension can counteract the ill-posedness we see in the WW2 and WW3 models is somewhat subtle. A study of the competition between dispersion and anti-diffusion that the first author and Wright have carried out for KdV-like equations in [12] (and see also Akhunov [13]) gives some clues to the present situation. It is found in references [12,13] that the Kato smoothing effect from the dispersive terms must be strong enough to counteract the growth inherent in the anti-diffusion. In the shallow-water KdV case, there is a loss of one derivative from the anti-diffusion (the anti-diffusion comes from a second derivative term of

indeterminate sign, leading to terms in the energy estimates with one more derivative than can be controlled through a naive estimate), but the Kato smoothing effect from the leading-order, dispersive term is also one derivative. Because the gain is as much as the loss, there is the possibility of balance, and initial-value problems can be well-posed if certain conditions are met.

The Kato smoothing effect for the full water-wave equations with surface tension has been found to provide a gain of a quarter of a derivative (see [14,15]) and the same is true for the WW2 and WW3 models. However, the term we have identified as making the primary contribution to ill-posedness is $(\Lambda\xi)^2$. In a naive energy estimate, this first-derivative term would throw up a quarter of a derivative *more than* can be controlled by the Kato smoothing. Because the loss of derivative is greater than the gain from Kato smoothing, it seems unlikely that the inclusion of the surface tension effect will substantially mitigate the ill-posedness described for truncated series models of water waves. In certain physical settings, such as in the case of hydro-elastic (or flexural) waves, the effect of dispersion is stronger (see, e.g. [16] or [17]). In this case, greater smoothing is likely to be available and hence a better chance of a well-posed, truncated series model.

It is worth remark, however, that on geophysical scales, if the model needs damping or surface tension for its well-posedness, then the model is suspect, independently of the theory. First, surface tension does not make a significant contribution on large spatial scales and damping is likewise not important unless the timescales are quite long. Second, we know for the full, deep water problem, the zero surface tension limit and the zero dissipation limit recover the unmodified problem (see [18,19] for the zero surface tension limit), whereas the evidence presented here points to this not being true for the truncated series models.

As mentioned already in §1, there are choices to be made when using the method of operator expansions to form a model. For example, instead of making expansions in the evolution equations, one may make expansions of the Hamiltonian, truncate this series and then derive evolution equations from the truncated Hamiltonian [20–23]. In [24], the well-posedness of some such models is considered, and it is argued that by including the effect of surface tension, a well-posed model can be formed. Again, we point out that if the model really needs to have surface tension effects included for well-posedness, then it is unlikely to be a good model on geophysical spatial and temporal scales.

Acknowledgements. D.M.A. thanks Paul Milewski and Michael Siegel for helpful conversations. D.M.A. gratefully acknowledges support from the National Science Foundation through grants nos. DMS-1008387 and DMS-1016267. Part of this work was done while J.L.B. was Professeur Invité at Université Bordeaux supported by INRIA. D.P.N. gratefully acknowledges support from the National Science Foundation through grant no. DMS-1115333.

Appendix A. Derivation of the model equations

We recall the formulation

$$\partial_t \eta = G(\eta)\xi \quad \partial_t \xi = -g\eta - R(\eta, \xi), \tag{A 1}$$

of the surface water wave problem, due originally to Zakharov [4]. Here, η is the deviation of the free surface from its rest position and ξ is the velocity potential evaluated at the free surface, while

$$R(\eta, \xi) = A(\eta)B(\eta, \xi) \text{ with } A(\eta) = \frac{1}{2(1 + (\partial_x \eta)^2)},$$
$$B(\eta, \xi) = (\partial_x \xi)^2 - (G(\eta)\xi)^2 - 2(\partial_x \xi)(\partial_x \eta)(G(\eta)\xi).$$

If $0 < \varepsilon \ll 1$ and

$$\eta(x, t) = \varepsilon f(x, t), \quad \xi(x, t) = \varepsilon q(x, t),$$

then a formal expansion in powers of ε is available, viz.

$$\{G(\eta), R(\eta,\xi), A(\eta), B(\eta,\xi)\} = \{G(\varepsilon f), R(\varepsilon f, \varepsilon q), A(\varepsilon f), B(\varepsilon f, \varepsilon q)\}$$
$$= \sum_{n=0}^{\infty} \{G_n(f), R_n(f,q), A_n(f), B_n(f,q)\}\varepsilon^n.$$

Approximate equations for the water-wave system (A 1) are then obtained by truncating this series at a particular order. For instance, the series expansion may be viewed as

$$\partial_t \varepsilon f = G_0[\varepsilon q] + \mathcal{O}(\varepsilon^2), \quad \partial_t \varepsilon q = -g\varepsilon f + \mathcal{O}(\varepsilon^2).$$

Upon dropping the second- and higher-order terms, the WW1 model

$$\partial_t f = G_0[q], \quad \partial_t q = -gf,$$

emerges. This system simply reflects the deep-water limit of the linear dispersion relation. If second-order terms are retained, but third-order terms dropped, the WW2 model

$$\partial_t f = G_0[q] + G_1(f)[q], \quad \partial_t q = -gf - A_0 B_2(f,q),$$

appears, while keeping the third-order terms leads to the WW3 model,

$$\partial_t f = G_0[q] + G_1(f)[q] + G_2(f)[q],$$
$$\partial_t q = -gf - A_0 B_2(f,q) - A_0 B_3(f,q).$$

Note that $B_0 \equiv B_1 \equiv 0$ which is why they do not appear in the above models.

To be useful, formulae for G_0, G_1 and G_2 are needed. These are straightforwardly seen to be (see [25]),

$$G_0[q] = \Lambda q,$$
$$G_1(f)[q] = -\partial_x[f\partial_x q] - \Lambda[f\Lambda q],$$
$$G_2(f)[q] = -\partial_x\left[\left(\frac{f^2}{2}\right)\partial_x \Lambda q\right] - \Lambda\left[\left(\frac{f^2}{2}\right)\Lambda^2 q\right] - G_1(f)[f\Lambda q]$$
$$= -\partial_x\left[\left(\frac{f^2}{2}\right)\partial_x \Lambda q\right] - \Lambda\left[\left(\frac{f^2}{2}\right)\Lambda^2 q\right] + \partial_x[f\partial_x[f\Lambda q]] + \Lambda[f\Lambda[f\Lambda q]],$$

where $\Lambda = H\partial_x$ as before. Because $A = 1/2(1 + (\varepsilon\partial_x f)^2)$, it follows that $A + \varepsilon^2(\partial_x f)^2 A = 1/2$. Expanding the left-hand side of the last formula in powers of ε gives

$$\sum_{n=0}^{\infty} A_n \varepsilon^n + \varepsilon^2(\partial_x f)\sum_{n=0}^{\infty} A_n \varepsilon^n = \frac{1}{2}.$$

Equating at orders zero, one and two yields

$$A_0 = \tfrac{1}{2}, \quad A_1 = 0, \quad A_2 = -\tfrac{1}{2}(\partial_x f)^2.$$

In a similar manner, it is seen that

$$B(\varepsilon f, \varepsilon q) = (\partial_x \varepsilon q)^2 - (G(\varepsilon f)[\varepsilon q])^2 - 2(\partial_x \varepsilon q)(\partial_x \varepsilon f)(G(\varepsilon f)[\varepsilon q])$$
$$= \varepsilon^2(\partial_x q)^2 - \left(\sum_{n=0}^{\infty} G_n(f)[q]\varepsilon^{n+1}\right)^2 - 2\varepsilon^2(\partial_x q)(\partial_x f)\left(\sum_{n=0}^{\infty} G_n(f)[q]\varepsilon^{n+1}\right)$$
$$= \varepsilon^2(\partial_x q)^2 - \sum_{n=2}^{\infty}\sum_{m=0}^{n-2}(G_{n-m+2}(f)[q])(G_m(f)[q])\varepsilon^{n-2}$$
$$- 2\varepsilon^2(\partial_x q)(\partial_x f)\sum_{n=2}^{\infty} G_{n-2}(f)[q]\varepsilon^{n-2},$$

so that $B_0 \equiv B_1 \equiv 0$, as advertised,

$$B_2(f,q) = (\partial_x q)^2 - (G_0[q])^2 = (\partial_x q)^2 - (\Lambda q)^2$$

and

$$\begin{aligned} B_3(f,q) &= -2G_0[q]G_1(f)[q] - 2(\partial_x q)(\partial_x f)G_0[q] \\ &= -2(\Lambda q)\{-\partial_x[f\partial_x q] - \Lambda[f\Lambda q] + (\partial_x q)(\partial_x f)\}. \end{aligned}$$

In consequence of these formal ruminations, the WW2 model is, in detail,

$$\begin{aligned} \partial_t f &= \Lambda q - \partial_x[f\partial_x q] - \Lambda[f\Lambda q] \\ \partial_t q &= -gf - (\tfrac{1}{2})\{(\partial_x q)^2 - (\Lambda q)^2\}, \end{aligned}$$

while WW3 can be written out as

$$\begin{aligned} \partial_t f &= \Lambda q - \partial_x[f\partial_x q] - \Lambda[f\Lambda q] - \partial_x\left[\left(\frac{f^2}{2}\right)\partial_x \Lambda q\right] - \Lambda\left[\left(\frac{f^2}{2}\right)\Lambda^2 q\right] - G_1(f)[f\Lambda q] \\ \partial_t q &= -gf - (\tfrac{1}{2})\{(\partial_x q)^2 - (G_0[q])^2\} + (\Lambda q)\{\partial_x[f\partial_x q] - \Lambda[f\Lambda q] + (\partial_x q)(\partial_x f)\}, \end{aligned}$$

or, alternatively,

$$\begin{aligned} \partial_t f &= \Lambda q - \partial_x[f\partial_x q] - \Lambda[f\Lambda q] - \partial_x\left[\left(\frac{f^2}{2}\right)\partial_x \Lambda q\right] - \Lambda\left[\left(\frac{f^2}{2}\right)\Lambda^2 q\right] \\ &\quad - \partial_x\left[\left(\frac{f^2}{2}\right)\partial_x \Lambda q\right] - \Lambda\left[\left(\frac{f^2}{2}\right)\Lambda^2 q\right] + \partial_x[f\partial_x[f\Lambda q]] + \Lambda[f\Lambda[f\Lambda q]] \\ \partial_t q &= -gf - (\tfrac{1}{2})\{(\partial_x q)^2 - (G_0[q])^2\} + (\Lambda q)\{\partial_x[f\partial_x q] - \Lambda[f\Lambda q] + (\partial_x q)(\partial_x f)\}. \end{aligned}$$

References

1. Lannes D. 2013 The water waves problem: mathematical analysis and asymptotics. In *Mathematical surveys and monographs* (eds RL Cohen, RM Guralnick, MA Singer, B Sudakov, MI Weinstein), vol. 188. Providence, MA: American Mathematical Society.
2. Strauss WA. 2010 Steady water waves. *Bull. Am. Math. Soc.* **47**, 671–694. (doi:10.1090/S0273-0979-2010-01302-1)
3. Craig W, Sulem C. 1993 Numerical simulation of gravity waves. *J. Comput. Phys.* **108**, 73–83. (doi:10.1006/jcph.1993.1164)
4. Zakharov VE. 1968 Stability of periodic waves of finite amplitude on the surface of a deep fluid. *J. Appl. Mech. Tech. Phys.* **9**, 190–194. (doi:10.1007/BF00913182)
5. Coifman RR, Meyer Y. 1985 Nonlinear harmonic analysis and analytic dependence. In *Pseudodifferential operators and applications* (Notre Dame, Ind., 1984). Proc. Symp. Pure Math. no. 43, pp. 71–78. Providence, RI: American Mathematical Society.
6. Ambrose DM, Bona JL, Nicholls DP. 2012 Well-posedness of a model for water waves with viscosity. *Discrete Contin. Dyn. Syst. B* **17**, 1113–1137. (doi:10.3934/dcdsb.2012.17.1113)
7. Dias F, Dyachenko AI, Zakharov VE. 2008 Theory of weakly damped free-surface flows: a new formulation based on potential flow solutions. *Phys. Lett. A* **372**, 1297–1302. (doi:10.1016/j.physleta.2007.09.027)
8. Bona JL, Chen M, Saut J-C. 2002 Boussinesq equations and other systems for small-amplitude long waves in nonlinear dispersive media: part I. Derivation and linear theory. *J. Nonlinear Sci.* **12**, 283–318. (doi:10.1007/s00332-002-0466-4)
9. Bona JL, Chen M, Saut J-C. 2004 Boussinesq equations and other systems for small-amplitude long waves in nonlinear dispersive media: part II. Nonlinear theory. *Nonlinearity* **17**, 925–952. (doi:10.1088/0951-7715/17/3/010)
10. Bona JL, Weissler FB. 2001 Blow-up of spatially periodic complex-valued solutions of nonlinear dispersive equations. *Indiana Univ. Math. J.* **50**, 759–782. (doi:10.1512/iumj.2001.50.1865)

11. Gottlieb D, Orszag SA. 1977 Numerical analysis of spectral methods: theory and applications. In *CBMS-NSF Regional Conference Series in Applied Mathematics*, no. 26. Philadelphia, PA: Society for Industrial and Applied Mathematics.
12. Ambrose DM, Wright JD. 2013 Dispersion vs. anti-diffusion: well-posedness in variable coefficient and quasilinear equations of KdV-type. *Indiana Univ. Math. J.* **62**, 1237–1281. (doi:10.1512/iumj.2013.62.5049)
13. Akhunov T. 2013 Local well-posedness of quasi-linear systems generalizing KdV. *Commun. Pure Appl. Anal.* **12**, 899–921. (doi:10.3934/cpaa.2013.12.899)
14. Alazard T, Burq N, Zuily C. 2011 Strichartz estimates for water waves. *Ann. Sci. Éc. Norm. Supér.* **44**, 855–903.
15. Christianson H, Hur VM, Staffilani G. 2010 Strichartz estimates for the water-wave problem with surface tension. *Commun. Partial Diff. Equ.* **35**, 2195–2252. (doi:10.1080/03605301003758351)
16. Blyth MG, Părău EI, Vanden-Broeck J-M. 2011 Hydroelastic waves on fluid sheets. *J. Fluid Mech.* **689**, 541–551. (doi:10.1017/jfm.2011.451)
17. Toland JF. 2008 Steady periodic hydroelastic waves. *Arch. Ration. Mech. Anal.* **189**, 325–362. (doi:10.1007/s00205-007-0104-2)
18. Ambrose DM, Masmoudi N. 2005 The zero surface tension limit of two-dimensional water waves. *Commun. Pure Appl. Math.* **58**, 1287–1315. (doi:10.1002/cpa.20085)
19. Ambrose DM, Masmoudi N. 2009 The zero surface tension limit of three-dimensional water waves. *Indiana Univ. Math. J.* **58**, 479–521. (doi:10.1512/iumj.2009.58.3450)
20. Olver PJ. 1984 Hamiltonian perturbations of water waves. In *Contemporary Math* (ed. JE Marsden), vol. 28, pp. 231–249. Providence, MA: American Mathematical Society.
21. Watson KM, West BJ. 1975 A transport-equation description of nonlinear ocean surface wave interactions. *J. Fluid Mech.* **70**, 815–826. (doi:10.1017/S0022112075002364)
22. West BJ, Brueckner KA, Janda RS, Milder DM, Milton RL. 1987 A new numerical method for surface hydrodynamics. *J. Geophys. Res.* **92**, 11 803–11 824. (doi:10.1029/JC092iC11p11803)
23. Milder DM. 1990 The effects of truncation on surface-wave Hamiltonians. *J. Fluid Mech.* **217**, 249–262. (doi:10.1017/S0022112090000714)
24. Lushnikov PM, Zakharov VE. 2005 On optimal canonical variables in the theory of ideal fluid with free surface. *Physica D* **203**, 9–29. (doi:10.1016/j.physd.2005.02.010)
25. Nicholls DP, Reitich F. 2001 A new approach to analyticity of Dirichlet–Neumann operators. *Proc. Royal Soc. Edinburgh A* **131**, 1411–1433. (doi:10.1017/S0308210500001463)